

Parallel Synthesis of Potent, Pyrazole-Based Inhibitors of *Helicobacter pylori* Dihydroorotate Dehydrogenase

Tasir S. Haque,^{*,†} Seifu Tadesse,^{†,‡} Jovita Marcinkeviciene,[§] M. John Rogers,^{||,⊥} Christine Sizemore,^{||,⊥} Lisa M. Kopcho,[§] Karen Amsler,^{||,#} Lisa D. Ecret,^{||} Dong Liang Zhan,[†] Frank Hobbs,[†] Andrew Slee,^{||,#} George L. Trainor,[†] Andrew M. Stern,[§] Robert A. Copeland,[§] and Andrew P. Combs[†]

Department of Medicinal Chemistry, Department of Chemical Enzymology, and Antimicrobials Group, Bristol-Myers Squibb Company, Experimental Station, Route 141 and Henry Clay Road, Wilmington, Delaware 19880

Received March 11, 2002

The identification of several potent pyrazole-based inhibitors of bacterial dihydroorotate dehydrogenase (DHODase) via a directed parallel synthetic approach is described below. The initial pyrazole-containing lead compounds were optimized for potency against *Helicobacter pylori* DHODase. Using three successive focused libraries, inhibitors were rapidly identified with the following characteristics: $K_i < 10$ nM against *H. pylori* DHODase, sub- μ g/mL *H. pylori* minimum inhibitory concentration activity, low molecular weight, and > 10 000-fold selectivity over human DHODase.

Introduction

Helicobacter pylori is a Gram-negative microaerophilic bacterium that infects up to 50% of the world's human population.¹ *H. pylori* resides in the acidic surroundings of the stomach, utilizing a high urease enzyme activity to provide a locally alkaline environment. First reported in 1982, *H. pylori* has been implicated in numerous gastrointestinal disorders and is associated with gastric ulcers, gastritis, and gastric cancer.² The current treatment of *H. pylori* infections typically utilizes a multiple drug therapy involving at least one broad spectrum antibiotic (antimicrobial therapy) and a proton pump inhibitor (antisecretory therapy). However, a *H. pylori* specific antimicrobial would be very desirable; a specific agent should avoid many of the negative gastrointestinal side effects associated with a broad spectrum antibacterial resulting from eradication of the normal gastrointestinal flora.

Dihydroorotate dehydrogenase (DHODase) is involved in the de novo pyrimidine synthesis pathway in most prokaryotic and eukaryotic cells. DHODase catalyzes the oxidation of dihydroorotate to orotate (Figure 1), the fourth step in de novo pyrimidine biosynthesis.³ Two major families of DHODases have been described.⁴ A low degree of similarity exists between the sequences of the two families (usually $< 20\%$).⁵ The enzymes may be distinguished by their location and cofactor utilization. Family 1 is found in the cytosol, while family 2 is membrane-associated. *H. pylori* DHODase belongs to family 2, as do all other DHODase enzymes from Gram-negative bacteria and mammals. All family 2 enzymes identified to date make use of an endogenous flavin mononucleotide (FMN) redox cofactor and exogenous

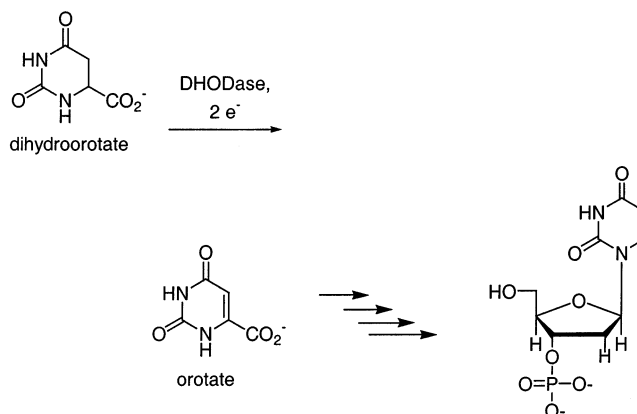


Figure 1. DHODase involvement in the pyrimidine biosynthetic pathway.

coenzyme Q₆ electron acceptor in the FMN oxidation half-reaction.⁶

As pyrimidines are crucial to the survival of the bacteria, it is not surprising to find that many organisms have pyrimidine salvage pathways, whereby pyrimidines may be generated by catabolism of nucleic acids and via salvage from exogenous sources of nucleotides. The genome sequences of two strains of *H. pylori* have been reported.^{7,8} Examination of the two genomes suggests that while the pathway for purine salvage is present in *H. pylori*, the pathway for pyrimidine salvage is, to a large extent, missing.⁶ If this salvage pathway is in fact absent, then *H. pylori* would be critically dependent on biosynthesis of pyrimidines; therefore, the pyrimidine pathway would be an attractive target for antibacterial therapy. DHODase is also present in mammalian cells. On the basis of previous research demonstrating that human DHODase could be inhibited with high selectivity over bacterial DHODase,⁹ we hypothesized that it would be possible to identify compounds that would selectively inhibit bacterial DHODase over the corresponding human enzyme.¹⁰ It should be noted that a high degree of selectivity over human DHODase is required, as inhibition of human

* To whom correspondence should be addressed. Tel: (302)467-6028. Fax: (302)467-6951. E-mail: Tasir.haque@bms.com.

[†] Department of Medicinal Chemistry.

[‡] Current address: Amgen, Inc., Thousand Oaks, CA 91320.

[§] Department of Chemical Enzymology.

^{||} Antimicrobials Group.

[⊥] Current address: National Institute of Allergy and Infectious Diseases, Bethesda, MD 20892.

[#] Current address: Enanta Pharmaceuticals, Watertown, MA 02472.

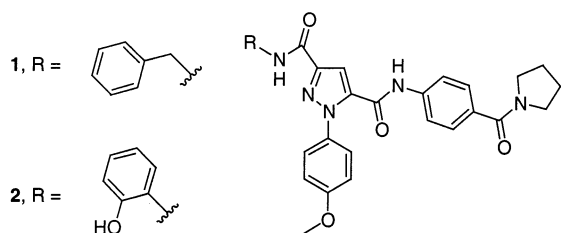


Figure 2. Pyrazole DHODase inhibitors **1** and **2**.

DHODase has been shown to have an immunosuppressive effect.^{11,12} Such an effect is clearly undesirable when combatting a bacterial infection.

We have previously reported the selective inhibition of bacterial DHODase by pyrazoles⁶ and thiadiazolidinediones.¹⁰ Pyrazole compounds **1** and **2** (Figure 2) were demonstrated to be potent inhibitors of *H. pylori* DHODase (K_i values against *H. pylori* DHODase of 26 and 50 nM, respectively, and minimum inhibitory concentration (MIC) of 3 $\mu\text{g}/\text{mL}$ vs *H. pylori* for compound **1**). These compounds are competitive with coenzyme Q_6 and were highly selective for *H. pylori* over human DHODase. In this paper, we discuss our efforts to improve upon the enzyme inhibition and antibacterial potency of the pyrazole series of compounds, beginning from lead compounds **1** and **2**.

Chemistry

After compounds **1** and **2** were identified as *H. pylori* DHODase inhibitors, we began to investigate the chemistry required for synthesis of analogues in a parallel format. The two amides off the central pyrazole in the lead compounds suggested natural starting places for disconnections. The core pyrazole could be accessed with one carboxylic acid protected as the ethyl ester, thus allowing the two coupling sites to be differentiated (Scheme 1). We chose to synthesize small, focused libraries so that information gained in the assay of a particular library could be incorporated into the planning of the subsequent library. An iterative approach also allowed the incorporation of a larger number of side chains at each position, without the exponential increase in the total number of compounds expected in a "true" combinatorial library. Additionally, we elected to use a pyrazole core that had been synthesized by "traditional" solution phase methods rather than assembling the pyrazole on a solid support. Synthesis of the core was accomplished with high selectivity for the desired regioisomer, which was then separated from any of the minor regioisomer by column chromatography. By using the isomerically pure pyrazole core and synthesizing the libraries in a spatially separate format, it was possible to unambiguously assign both the identity and the regiochemistry of all of our products. In contrast, most on-support synthetic approaches to the desired pyrazoles would have required a lengthy development time to obtain regiospecifically substituted products or would have resulted in a mixture of two regioisomers (requiring postassay analysis to determine the identity of the active regioisomer).

The side chain sets for the libraries were selected based on a combination of knowledge of medicinal chemistry and availability of reagents (from either

commercial suppliers or an in-house collection). Computational resources for this project were limited, so no structure-based or diversity selection computational methods were applied. Instead, the side chains were chosen to explore specific hypotheses regarding inhibitor binding (e.g., benzylamines in R^B set of library 2) or to maximize diversity at a position using readily available and chemically compatible reagents (e.g., R^A amine set of library 1).

The synthesis of the first library was carried out as shown in Scheme 1. The first amine side chain (R^A) was attached to backbone amide linker (BAL)-linked polystyrene resin via a reductive amination. The monoacid/monoester pyrazole core containing R^C was then coupled to the amine, after which the ester was saponified with LiOH in tetrahydrofuran (THF)/ $\text{H}_2\text{O}/\text{MeOH}$. Finally, the second amine side chain (R^B) was coupled to the pyrazole acid, and the resulting product was cleaved from the polymer support using trifluoroacetic acid.

All compounds were examined by analytical high-performance liquid chromatography (HPLC) chromatography (detecting at 220 and 254 nm) and flow injection mass spectrometry following cleavage from solid support, whereupon it was discovered that 43 of the desired 120 compounds were not obtained in amounts sufficient for biological assay. Comparison of the products obtained to those that failed showed that the poor yields were correlated to the use of anilines at R^A . For example, 4-aminopyridine (A6, shown in Figure 4) failed with all R^B combinations. After several test reactions were conducted with anilines, we noted that while the reductive amination of anilines to the aldehyde linker proceeded smoothly, subsequent coupling of the pyrazole to the secondary aniline (using standard *O*-(7-azabenzotriazol-1-yl)-*N,N,N,N*-tetramethyluronium hexafluorophosphate (HATU) coupling conditions) gave poor yields of the desired amide. We chose to purify this first library, obtain as many of the desired products as possible, and then revisit our approach to the synthesis of solid phase pyrazole libraries.

The pyrazole synthesis on solid support was optimized to allow for incorporation of anilines at the R^A position in library 2. After a variety of coupling reagents and conditions were tried, double coupling of the resin-bound amine at 50 °C using PyBrOP as the coupling reagent was found to provide a high yield (75–90%) of the support-bound pyrazole product (Figure 3). In both the second and the third libraries, PyBrOP was used whenever a pyrazole acid was coupled to a support-bound aniline, and HATU was used for coupling a pyrazole acid to a support-bound alkylamine.

We concurrently developed an alternate synthetic approach to aniline-substituted pyrazole amides, whereby the furan-protected pyrazole acid could be coupled onto support and then oxidized to the carboxylic acid to liberate the second coupling site (Figure 3). In this route, the R^B side chains are initially reductively aminated onto the support, and the R^A side chain is coupled in the final step before cleavage. Coupling of the primary aniline to the support-bound carboxylic acid would allow for the incorporation of anilines at R^A , as the difficulties with the aniline coupling were only observed when the aniline was attached to the linker. However, a small loss in yield of the final products was observed in this

Scheme 1. Support-Bound Synthesis of Pyrazoles

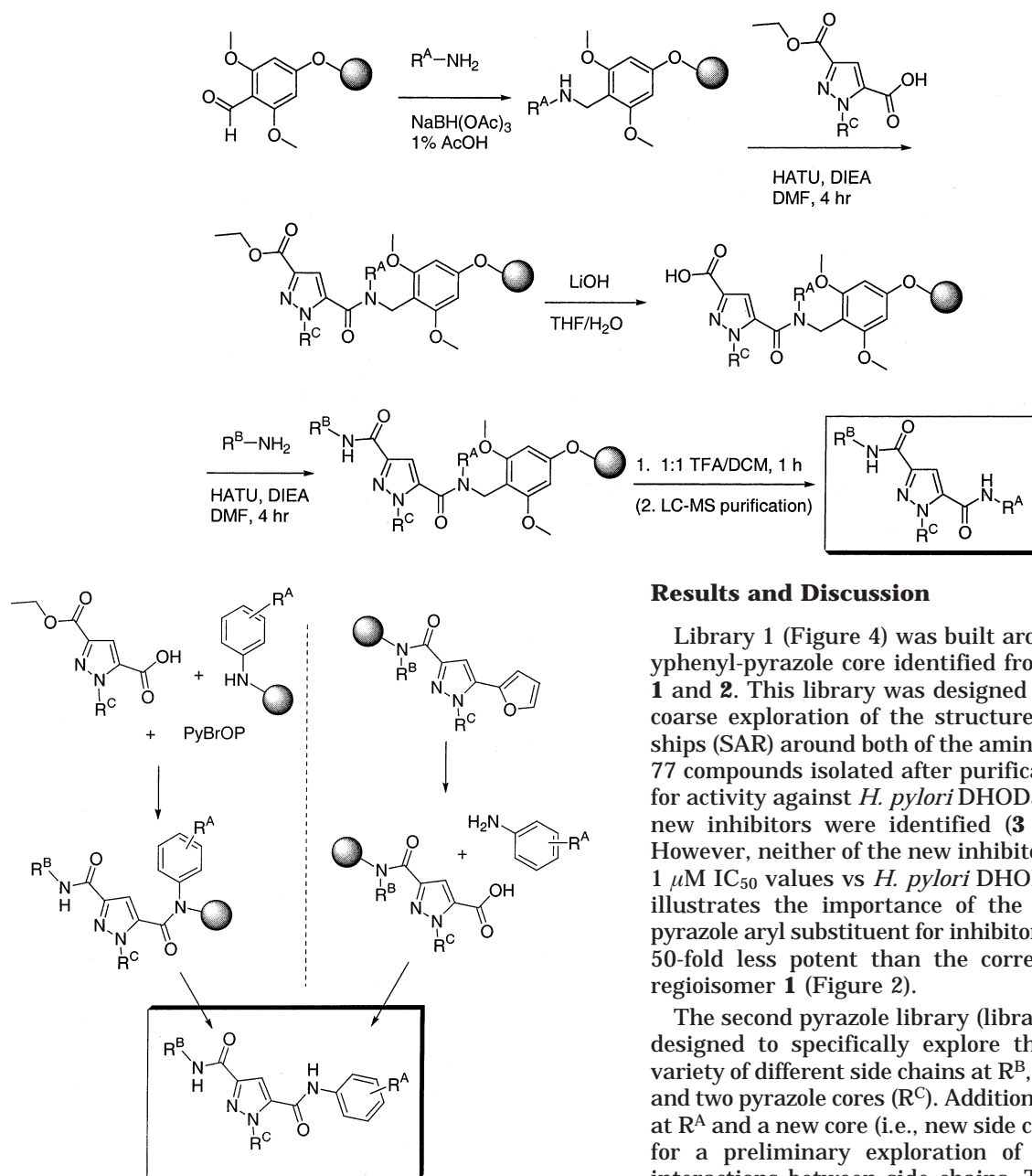


Figure 3. Two synthetic routes for accessing aniline-containing R^A side chains. In the left route, PyBrOP is used to couple the pyrazole acid to the support-bound aniline; in the right route, the aniline is coupled to the support-bound pyrazole after $RuCl_3$ -catalyzed oxidation of the furan to the carboxylic acid.

route, possibly due to cleavage during the oxidation step. A mild reduction in purity was also observed in several cases where oxidation of the furan to the carboxylic acid was incomplete.

The first method described above (use of PyBrOP as coupling reagent) permits the inclusion of anilines at both R^A and R^B positions without changing the core pyrazole used in the synthesis. We also found complete hydrolysis of the support-bound ester to the carboxylic acid to be more reliable than complete oxidation of the support-bound furan to the carboxylic acid. For these two reasons, the more versatile PyBrOP coupling reagent route was chosen for libraries 2 and 3.

Results and Discussion

Library 1 (Figure 4) was built around the 4-methoxyphenyl-pyrazole core identified from lead compounds **1** and **2**. This library was designed to provide a rapid, coarse exploration of the structure–activity relationships (SAR) around both of the amine substituents. The 77 compounds isolated after purification were assayed for activity against *H. pylori* DHODase (Figure 5). Two new inhibitors were identified (**3** and **4**, Figure 6). However, neither of the new inhibitors had better than 1 μM IC₅₀ values vs *H. pylori* DHODase. Compound **3** illustrates the importance of the orientation of the pyrazole aryl substituent for inhibitory activity, as **3** was 50-fold less potent than the corresponding pyrazole regioisomer **1** (Figure 2).

The second pyrazole library (library 2, Figure 7) was designed to specifically explore the R^B site, with a variety of different side chains at R^B , two R^A side chains, and two pyrazole cores (R^C). Addition of a new side chain at R^A and a new core (i.e., new side chain at R^C) allowed for a preliminary exploration of potential additive interactions between side chains. The R^B side chains were selected in order to probe the binding pocket of the benzyl side chain. Synthesis of library 2 was high yielding (70–95%) and quite clean, with product purities uniformly in excess of 80% (as determined by HPLC/UV detection at 254 nm and examination of product ¹H NMR spectra). Therefore, the library was assayed for inhibitory activity without further purification, and selected active inhibitors were resynthesized, purified, and reevaluated. A very good correlation between K_i values obtained with unpurified and purified material was observed for this series of compounds.

A number of compounds from this second library were inhibitors of *H. pylori* DHODase; 18 compounds had inhibitory activity at concentrations under 11 μM , with 7 of the 18 having K_i values between 10 and 100 nM. When R^B was 4-fluorobenzyl (B17), little change in enzyme inhibition (vs compound **1**) was observed, but as the R^B para substituent increased in size (chloro to methoxy to cyclohexyl), there was a corresponding

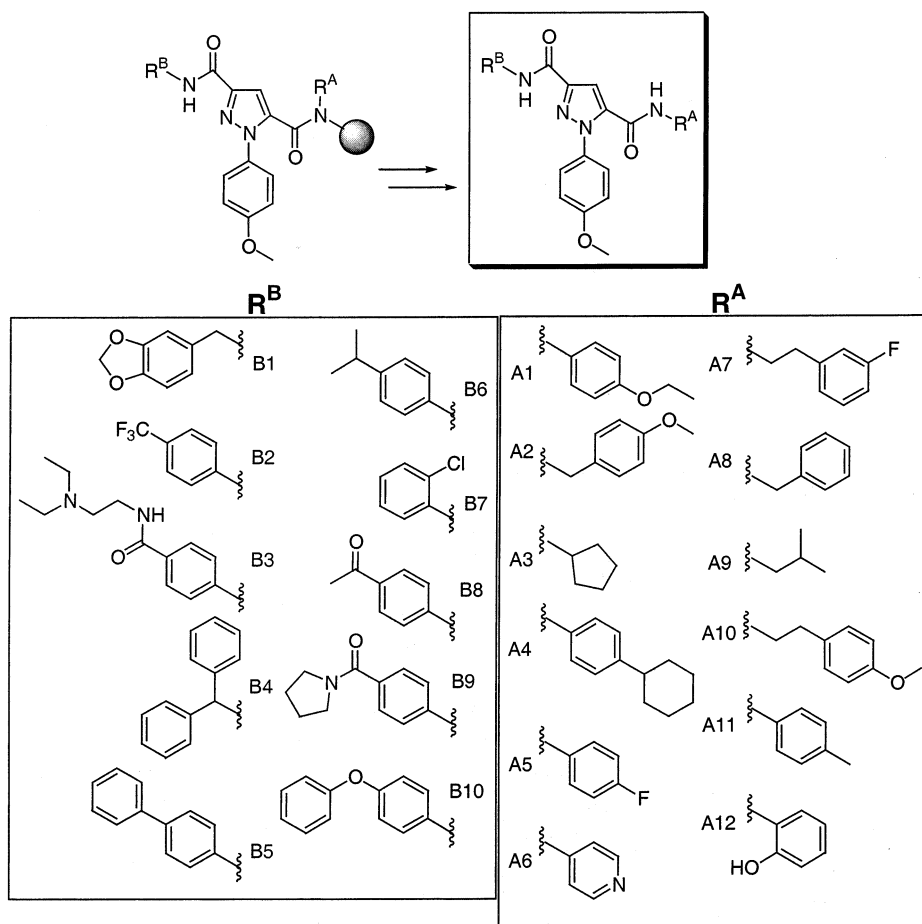


Figure 4. Side chains for pyrazole library 1.

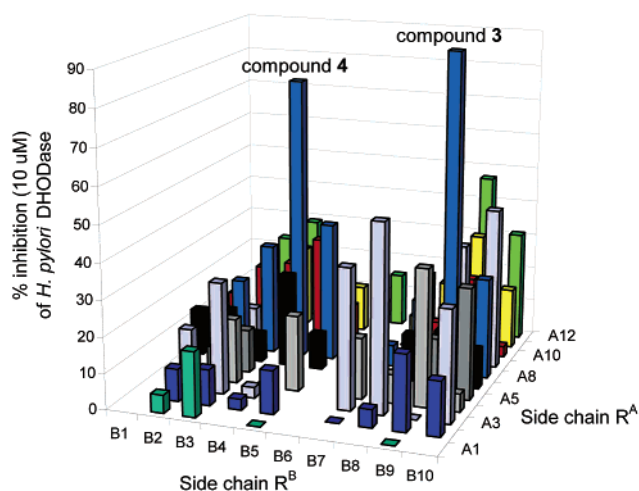


Figure 5. Graph of library 1, % inhibition (at 10 μ M compound) of *H. pylori* DHODase vs side chains R^A and R^B .

decrease in potency. Analogues with aromatic side chains at R^B were considerably more potent DHODase inhibitors than analogues with $R^B =$ alkyl side chains. For example, compare the activity of the benzyl R^B side chain in **1** (A13:B15:C1, 26 nM) with the two most potent alkyl R^B replacements, isobutyl (compound **5**, A13:B11:C1, 138 nM) or tetrahydrofuryl (racemic compound **6**, A13:B13:C1, 331 nM), Table 1.

The $R^C =$ 4-methoxyphenyl (C1) inhibitors in general were more potent than the corresponding $R^C =$ phenyl (C2) inhibitors, especially for mildly potent compounds

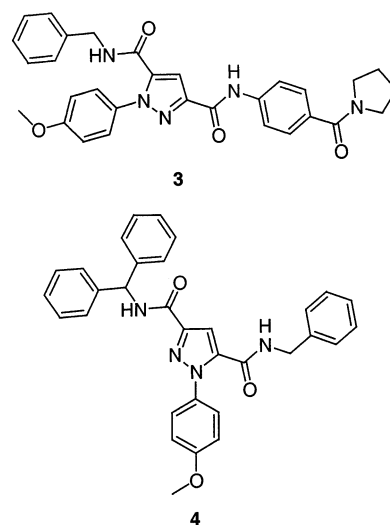


Figure 6. Compounds **3** ($R^A = A8$, $R^B = B9$) and **4** ($R^A = A8$, $R^B = B4$) from library 1. Note that **1** (Figure 1) and **3** are regioisomers around the pyrazole core.

(e.g., 331 nM for A13:B13:C1 vs 4400 nM for A13:B13:C2). At the R^A position, the 4-(pyrrolidine-1-carbonyl)-phenyl substituent A13 was clearly superior to the cyclopentyl substituent A3, with none of the compounds containing the latter R^A substituent having inhibitory activity better than 10 μ M vs *H. pylori* DHODase.

All compounds from library 2 were evaluated for whole cell activity vs *H. pylori*. MIC was determined against a reference American Type Culture Collection

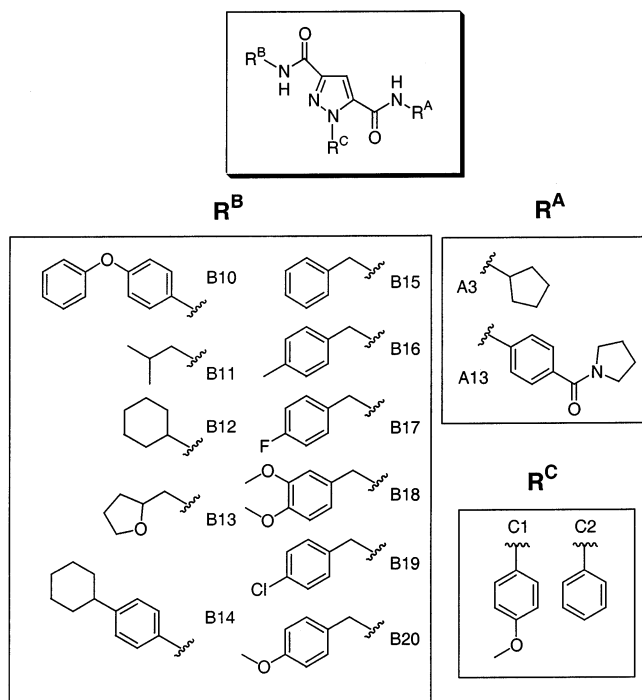


Figure 7. Side chains for pyrazole library 2.

(ATCC) strain of *H. pylori* under standard conditions. As discussed above, numerous inhibitors with K_i values lower than $1 \mu\text{M}$ against the *H. pylori* DHODase enzyme were identified. However, as compared to lead compound **1**, none of the library 2 compounds had an improved activity ($<3 \mu\text{g/mL}$) vs *H. pylori* bacteria in the whole cell assay.

For our final directed library (Figure 8), we focused our attention on the R^A side chain. It was believed that reduction of the molecular weight of the inhibitors and incorporation of pyridine side chains at R^B might result in compounds with more desirable physical characteristics. By decreasing the size of the molecules and adding aromatic or tertiary amines, aqueous solubility and cell permeability of the compounds may be improved, potentially resulting in greater antimicrobial potency. Several side chains were selected to determine which characteristics of the somewhat large A13 side chain were necessary for tight binding to *H. pylori* DHODase. We were also able to examine several other side chains at R^A and R^B , while still focusing on benzyl derivatives at R^C . This allowed us to probe for additive effects between sites, while synthesizing a relatively small number of compounds (160 members in library 3). All products from the third library were purified by preparative liquid chromatography/mass spectrometry (LC/MS) prior to biological assay.

There were a number of potent ($K_i < 100 \text{ nM}$) compounds identified in library 3 (see Table 2). It is clear that the A13 side chain can be truncated all the way down to the unsubstituted aniline side chain (A14) at the R^A position with no loss of inhibitory potency (Table 3, compounds **7** and **8**). The structural constraint introduced by the amide in the A13 side chain is not necessary for activity, as demonstrated by compound **9** with the extended A18 side chain ($K_i = 8 \text{ nM}$, A18:B22:C3). However, replacement of the aniline with an alkyl side chain at R^A (e.g., A9, A15, or A16) resulted in a

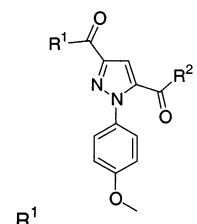
significant decrease in inhibition ($K_i = 91 \text{ nM}$ for **10**, A9:B15:C3).

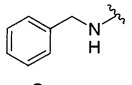
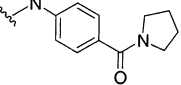
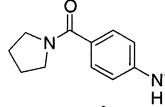
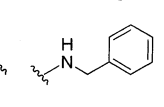
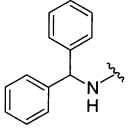
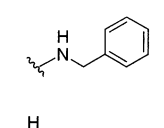
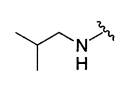
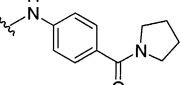
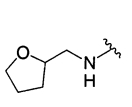
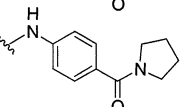
At the R^B position, the (3-aminomethyl)pyridine (B22, Table 3, **11**) or unsubstituted benzylamine (B15, Table 3, **8**) side chains were preferred over the 3- or 4-methyl-substituted benzylamine side chains (B16 and B21, Table 3, **12**). At the R^C position, the 4-chlorophenyl substituent (C3) was consistently favored over the 4-methoxyphenyl (C1) or unsubstituted phenyl (C2) substituent. For example, compare Table 3, compounds **11** and **13**. Finally, all of the compounds containing a methyl R^C substituent (C4) were inactive against *H. pylori* DHODase. For the pyrazole substituent (R^C), the general order of activity was 4-chlorophenyl > 4-methoxyphenyl > phenyl \gg methyl.

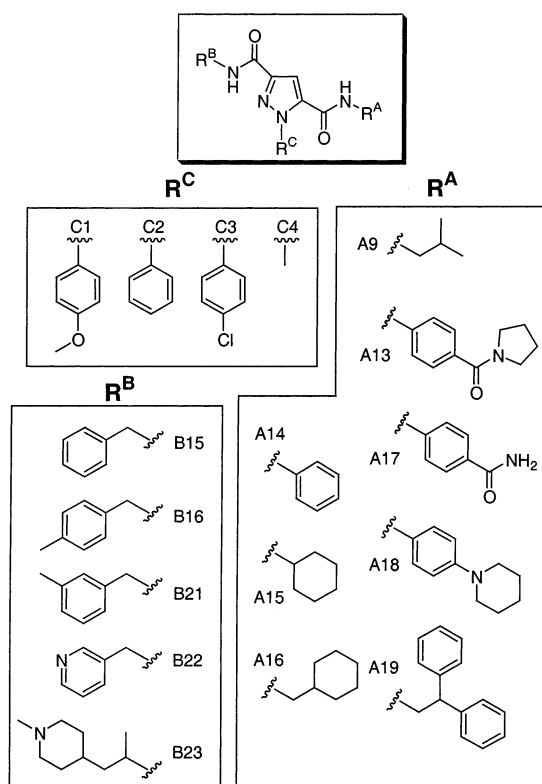
Several compounds with good whole cell activity vs *H. pylori* were identified from library 3. Compounds **8** and **11** (MIC values of 0.125 and $0.250 \mu\text{g/mL}$, respectively) were the most potent compounds identified both in terms of DHODase inhibition and activity in the MIC assay. These compounds were of sufficient antibacterial potency that they could be carried forward into a proof of principle study. Preliminary data suggest that *H. pylori* growth cannot recover after treatment of the organism with these inhibitors and subsequent compound removal. These results suggest that the compounds act as bactericidal agents; however, this conclusion must be viewed with some caution because of the very slow growth rates of *H. pylori* in cell culture.

To define further the whole cell activity of the pyrazole-based compounds, spontaneous resistant mutants of *H. pylori* were obtained at $4\times$ and $8\times$ MIC levels of compound **1**. These resistant mutants were obtained at a frequency of approximately $(1-2) \times 10^{-7}$ viable *H. pylori* cells plated for both the ATCC strain 43629 and the SS1 strain,¹³ implying that a single target is the site of action for compound **1**.¹⁴ The resistance was determined to be at high levels of **1** ($>64 \mu\text{g/mL}$). Genomic DNA was prepared, and the *pyrD* gene was amplified from several of these resistant mutants. In multiple isolates, a common mutation C \rightarrow A was determined, changing codon 18 from GCG \rightarrow GAG, corresponding to an Ala \rightarrow Glu mutant enzyme (A18E). To confirm this, the C \rightarrow A change was introduced by in vitro mutagenesis of the wild-type enzyme. The mutant and wild-type *H. pylori* enzymes were cloned and overproduced in a *pyrD* mutant of *Escherichia coli*, so there was no contamination of endogenous *E. coli* DHODase activity.¹⁵ Purification and biochemical analysis of the mutant A18E DHODase revealed that while the kinetic parameters for the dihydroorotate substrate and coenzyme Q_0 were unchanged, the K_i for compound **1** was elevated 6-fold. The increase in K_i is less than the increase in MIC (at least 8-fold) for the resistant mutants. However, the reported toxicity of upstream intermediates in the pathway¹⁶ and the overall effect of inhibition of the pathway for pyrimidine biosynthesis on cell growth were not considered in the assay of the single enzyme. These factors may account for the observed differences between the changes in K_i and MIC values.

DHODase has also been identified as the target of an antifungal compound in *Aspergillus nidulans*.¹⁷ In this case, moderate and high level resistant mutants were

Table 1. Selected Actives from Libraries 1 and 2


R ¹	R ²	Compound	<i>H. pylori</i> DHODase K _i (nM)	<i>H. pylori</i> MIC (μg/mL)	Human DHODase K _i (nM)
		1	26	3	>50,000
		3	1500	>32	>50,000
		4	2400	>32	>50,000
		5	138	64	>50,000
		6	331	>32	>50,000

**Figure 8.** Side chains for pyrazole library 3.

obtained from several mutations; the high level resistant enzyme was about 2500 times less sensitive to the inhibitor as measured by IC₅₀ determination in crude enzyme preparations. An alignment of DHODase enzymes shows that the A18E mutation in the *H. pylori* enzyme is close to a corresponding histidine 26 mutation, defined by alanine scanning as affecting brequinar

Table 2. Comparison of Number of Active Compounds (within Three Potency Ranges) in the Three Pyrazole Libraries

library	size (no. of compds)	1 μM < K _i < 10 μM	100 nM < K _i < 1 μM	K _i < 100 nM
1	77	2	0	0
2	44	7	4	7
3	160	5	6	31

binding in the human DHODase enzyme.¹⁵ These data support the *N*-terminal portion of the enzyme in cofactor binding and specificity in interactions with inhibitors, supported by the recent description of the X-ray crystallographic structure of human DHODase with inhibitors.¹⁸

A spontaneously resistant mutant of *H. pylori* was obtained with compound **13** using a method analogous to that described above. Each mutant was then tested for cross-resistance to the pyrazole not used to develop the strain. (For example, the MIC of compound **1** was determined for the mutant developed using compound **13**.) As shown in Table 4, a high level of cross-resistance between the strains derived from the two pyrazoles was observed. This result suggests that bacterial isolates resistant to one pyrazole inhibitor will be resistant to the other pyrazole inhibitors identified above. The onset of spontaneous resistance in vitro to compound **1** was rapid, and cross-resistance to other members of the inhibitor class is high, suggesting a liability to the pyrazoles as potential *H. pylori* therapeutic agents.

Conclusion

A number of potent *H. pylori* DHODase inhibitors based upon a pyrazole core were identified. Directed parallel synthesis enabled the rapid optimization of lead compounds via three focused libraries. All of the libraries discussed above were developed, synthesized, and

Table 3. Selected Inhibitors from Library 3

				Compound	H. pylori DHODase K_i (nM)	H. pylori MIC ($\mu\text{g/mL}$)	Human DHODase K_i (nM)
			7	6	8	>50,000	
			8	4	0.125	50,000	
			9	8	2	>50,000	
			10	91	>64	>50,000	
			11	4	0.250	>50,000	
			12	32	32	>50,000	
			13	12	0.500	>50,000	

Table 4. MIC of Compounds **1** and **13** vs Wild Type and Resistant *H. pylori* Isolates

compd	wild type MIC ($\mu\text{g/mL}$)	1 resistant isolate MIC ($\mu\text{g/mL}$)	13 resistant isolate MIC
1	3.00	>64	>64
13	0.50	32	24

purified by two chemists in 9 months. The most potent DHODase inhibitors are very selective (>10 000-fold) for *H. pylori* over human DHODase enzymes. The inhibitors display low $\mu\text{g/mL}$ to sub- $\mu\text{g/mL}$ antibacterial activity against *H. pylori*. However, no antibacterial activity is seen against a variety of other Gram-positive and Gram-negative organisms (*Staphylococcus aureus*, *Enterococcus faecalis*, *Streptococcus pyogenes*, *E. coli*, *Haemophilus influenzae*, *Moraxella catarrhalis*, and *Pseudomonas aeruginosa*). The authors speculate that this selectivity is due to the absence of a pyrimidine salvage pathway in *H. pylori* and the presence of an active pathway in the other organisms. Compounds **8** and **11** are the most potent DHODase enzyme inhibitors identified ($K_i = 4$ nM for both). Both compounds were also very active against *H. pylori* in a whole cell antimicrobial assay (MIC = 0.125 $\mu\text{g/mL}$ for **8**, 0.250 $\mu\text{g/mL}$ for **11**). The pyrazoles have a high level of spontaneous resistance (on the order of $(1-2) \times 10^{-7}$ viable *H. pylori* cells) as well as cross-resistance within the class, suggesting a single target as the site of action resulting in whole cell activity.

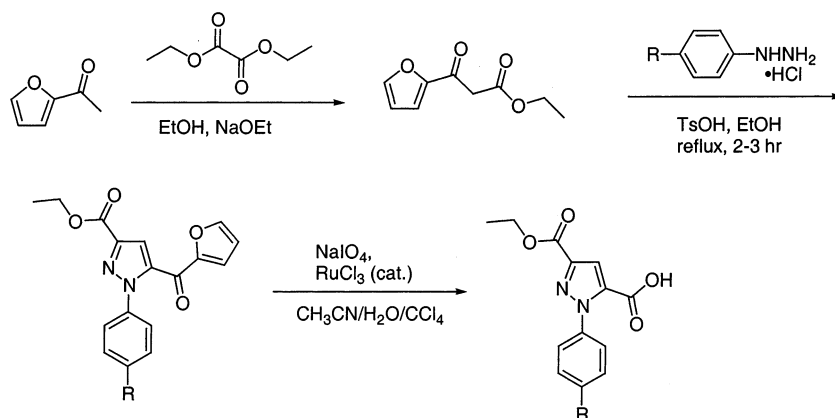
The synthesis of the first two small libraries allowed us to rapidly identify motifs important to enzyme inhibitor potency. This knowledge was incorporated into the design of the third library. The third library was devised with the goal of finding multiple potent DHODase inhibitors. These could then be screened for whole cell activity against *H. pylori*. We favored the approach of finding many potent inhibitors and screening for the whole cell activity in our third library, rather than trying to optimize whole cell activity in an iterative, stepwise fashion. As shown in Table 2, library 3 demonstrates the utility of this approach: library 3 contained 31 compounds with K_i values under 100 nM, several of which possessed potent whole cell activity. We believe that a similar strategy could be successful for a variety of medicinal targets, where the generation of large numbers of potent compounds in later libraries would allow for selection of compounds having desirable biological and pharmacological characteristics.

Experimental Section

Enzymology/Biology. Protein Expression and Purification. *H. pylori* and human DHODase were expressed and purified as previously described.⁶ A full description is provided in the Supporting Information accompanying this paper.

Enzymatic Activity Assays, Inhibition Studies, and Cellular Studies. Human and *H. pylori* enzymatic activity assays and inhibition studies and *H. pylori* cellular studies were performed as previously described.⁶

Chemistry. Intermediates were monitored by thin-layer chromatography (silica gel plates), flow injection positive ion

Scheme 2. Synthesis of Pyrazole Cores

electrospray mass spectrometry using a Micromass ZMD quadrupole mass spectrometer, and HPLC on a Varian Prostar instrument (eluting with acetonitrile/water through a 4.6 mm \times 50 mm C-18 column and monitoring at 220 and 254 nm). Final products of support-bound syntheses were characterized by flow injection positive ion electrospray mass spectrometry, by HPLC (254 nm detection), and by ^1H LC NMR with a Varian Inova 400 MHz NMR spectrometer equipped with a 60 μL active volume flow probe and a Gilson 215 liquids handler, using 3:1 $\text{DMSO-}d_6/\text{CDCl}_3$ as solvent. NMR spectra of compounds synthesized in solution were obtained on a Varian VXR/Unity 300 MHz spectrometer. Elemental analysis of products was performed by Quantitative Technologies, Inc. Pyrazole cores and library compounds were synthesized from commercially available starting materials and solvents.

Solution Phase Synthesis of Pyrazole Cores. The pyrazole monoacid/monofuran cores were synthesized as previously described (as shown in Scheme 2).¹⁹ Reaction of the appropriate hydrazine and 2-furanpropanoic acid, β -oxo-, ethyl ester in the presence of acetic acid resulted in the desired pyrazole ester in good to high regioselectivity.²⁰ The product was then further purified by crystallization or silica gel flash chromatography to provide the desired pyrazole as a single regioisomer. Finally, the furan was oxidized to the carboxylic acid as previously reported, with sodium periodate and ruthenium(III) chloride²¹ or potassium permanganate to provide (after purification) the desired pyrazole acid/ester in 55–85% yield.

Support-Bound Synthesis of Pyrazoles. The pyrazoles were synthesized on polystyrene beads using Robbins filtration blocks.²² Amines were reductively aminated onto a BAL linker, resulting in a support-bound secondary amine. Monoacid/monoester pyrazole cores were then coupled to the secondary amines using PyBrOP. The resulting support-bound ethyl ester was hydrolyzed with LiOH in THF/ H_2O /MeOH. Finally, the second amine was coupled to the pyrazole acid, resulting in the desired products. Pyrazoles were cleaved into 2 mL 96 well plates using TFA/ CH_2Cl_2 . A representative procedure (used for synthesis of the second library, including both resin-bound amines and anilines) is given below.

Step 1. Reductive Amination of Amine onto PS-BAL Resin. The primary amine (or aniline) was dissolved in a mixture of 1% acetic acid in DMF to afford a solution that was 0.2 M in amine. To this solution was added sodium triacetoxyborohydride (0.2 M final concentration). The solution was immediately added to 1.00 g of PS-PEG-BAL (polystyrene-poly(ethylene glycol)-(4-formyl-3,5-dimethoxyphenyl)) resin (initial loading = 0.55 mmol/g) in a fritted tube. The reaction was mixed several times over 1 h, and then, the tube was capped, placed on an orbital shaker, and allowed to stir overnight (15 h). The solution was then drained from the resin, and the resin was washed with methanol (1 \times), 10% *N,N*-diisopropylethylamine (DIEA) in DMF (2 \times), DMF (7 \times), CH_2Cl_2 (7 \times), methanol (3 \times), and CH_2Cl_2 (3 \times). The resin was then dried in vacuo. Completion of reaction was determined by solid phase ^1H NMR of the resin.

Step 2A. Coupling of Pyrazole Carboxylic Acid Cores onto Resin-Bound Secondary Amines.

The resin-bound amine from step 1 was distributed into two fritted tubes (one for each of the two pyrazole cores), 0.500 g/tube. One of the pyrazole cores was dissolved in DMF to afford a 0.45 M solution. To this solution was added 2 equiv of DIEA, followed by 1 equiv of HATU. The resulting solution was added to the tubes containing resin-bound amine. The tubes were capped and agitated on an orbital shaker for 4 h (running the reaction overnight afforded no advantage). The solution was drained from the resin, and the resin was washed with DMF (5 \times), methanol (5 \times), and CH_2Cl_2 (7 \times). Reaction completion was determined by ninhydrin test and by cleaving a small portion (20–30 mg) of resin with 1:1 TFA/ CH_2Cl_2 for 1 h and then checking by ES-MS and HPLC. Acylation was typically complete after one coupling reaction, but if necessary, a second coupling reaction was performed to fully acylate the resin-bound amine.

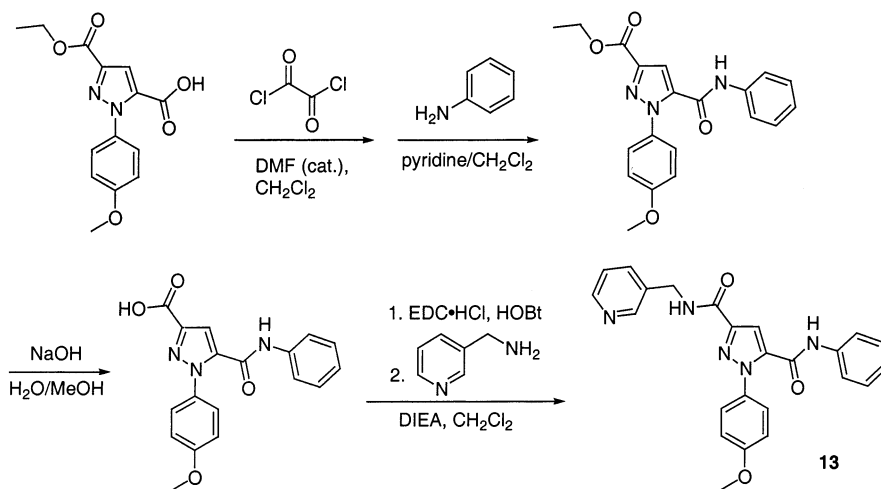
Step 2B. Coupling of Pyrazole Carboxylic Acid Cores onto Resin-Bound Secondary Anilines.

The resin-bound amine from step 1 was distributed into two vials (one for each of the two pyrazole cores), 0.500 g/vial. Each of the pyrazole cores was dissolved in DMF to afford two 0.45 M solutions. To each solution was added two equiv of DIEA, followed by 1 equiv of PyBrOP (bromo-tris-pyrrolidino-phosphonium hexafluorophosphate). The resulting solution was added to one of the vials containing resin-bound amine. The vial was capped, placed in a 50 $^\circ\text{C}$ sand bath, and agitated on an orbital shaker for 2 h. The suspension containing the resin was transferred to a fritted tube, drained, and rinsed with DMF (3 \times). The resin was transferred back into a glass vial, and the coupling reaction was then repeated using the same conditions as above (PyBrOP, DIEA in DMF, 50 $^\circ\text{C}$, 2 h). The suspension containing the resin was transferred to a fritted tube and drained, and the resin was washed with DMF (5 \times), methanol (5 \times), and CH_2Cl_2 (7 \times). Reaction completion was determined by ninhydrin test and by cleaving a small portion (20–30 mg) of resin with 1:1 TFA/ CH_2Cl_2 for 1 h and then checking for product formation by ES-MS and HPLC.

Step 3. Hydrolysis of Support-Bound Ethyl Ester.

Lithium hydroxide (5 equiv relative to resin loading) was dissolved in a THF/MeOH/ H_2O mixture (5:2:2 ratio, 0.1 M LiOH final concentration). The resulting solution was added to the resin-bound ester in the Robbins blocks. The blocks were then sealed and agitated for 4 h at room temperature. The wells were then drained, and the resin was washed with THF (4 \times), H_2O (5 \times), MeOH (5 \times), and CH_2Cl_2 (7 \times). A small portion of resin was cleaved, and the reaction progress was checked by mass spectrometry and HPLC. Hydrolysis of resin-bound ester was spectroscopically complete after one treatment with LiOH.

Step 4. Coupling of Amines or Anilines onto Resin-Bound Pyrazole Carboxylic Acid Cores. A 9 equiv amount of DIEA and 4.5 equiv of HATU (for amine nucleophiles) or 4.5 equiv of PyBrOP (for aniline nucleophiles) were dissolved in enough DMF to yield a solution that was 0.1–0.2 M in coupling reagent. The resulting solution was added to the

Scheme 3. Solution Phase Synthesis of Compound **11** (Standard Solution Phase Scale-Up Method)

Robbins block wells containing resin-bound carboxylic acid. The acid was preactivated with the coupling reagent for 10–15 min. The desired amine or aniline was then added to the appropriate wells (in a minimal amount of DMF, if needed). The block was then sealed and agitated on an orbital shaker overnight. The solution was drained from the resin, and the resin was washed with DMF (7×), methanol (5×), and CH₂-Cl₂ (7×). Reaction completion was determined by cleaving a small portion (20–30 mg) of resin with 1:1 TFA/CH₂Cl₂ for 1 h and then checking by ES-MS and HPLC. Coupling to the resin-bound acid was typically complete after one reaction, but if necessary, a second coupling reaction was performed to fully react the resin-bound acid to the desired amide.

Step 5. Cleavage of Product from Solid Support. Products were cleaved from Robbins blocks directly into 2 mL 96 well plates. To each well was added 0.70 mL of 1:1 trifluoroacetic acid/CH₂Cl₂. After 1 h, the cleavage solution was drained into a 2 mL 96 well plate, and the resin was washed with 0.5 mL of CH₂Cl₂. The wash solution was combined with the cleavage solution, and the samples were evaporated to dryness.

Step 6. Purification of Library Products. When necessary, compounds were purified by LC/MS on a Waters Micromass instrument, collecting on the expected product molecular weight. Compounds purified by LC/MS were collected via mass-directed fractionation using a Micromass ZMD mass spectrometer and Gilson 306 LC pumps, with fraction collection controlled by Micromass Fractionlynx software. Fractions containing product were evaporated to dryness, and products were characterized by analytical LC/MS and ¹H NMR.

Solution Phase Scale-Up of Pyrazole Products. In nearly all cases, products were either scaled up on support using a larger quantity of resin or in solution using analogous techniques (for example, see synthesis of compound **13** in Scheme 3). In solution, anilines were coupled via generation of the appropriate acid chloride, while amines were coupled via the acid chloride or the 1-hydroxybenzotriazole-activated ester (generated with EDC·HCl). One exception was compound **7**, which was scaled up in solution using 4-aminobenzonitrile (coupling via the mixed anhydride generated with POCl₃²³) and then hydrolyzing the nitrile to the primary amide with sodium bicarbonate²⁴ (see Scheme 4 in Supporting Information).

Compound 1. ¹H NMR (300 MHz, CDCl₃): δ 1.83–1.96 (m, 4 H), 3.37 (t, *J* = 6.3 Hz, 2 H), 3.62 (t, *J* = 6.8 Hz, 2 H), 3.82 (s, 3 H), 4.57 (d, *J* = 6.2 Hz, 2 H), 6.94 (d, *J* = 9.1 Hz, 2 H), 7.23–7.41 (m, 10 H), 7.64 (d, *J* = 8.4 Hz, 2 H), 7.70 (s, 1 H), 9.57 (s, 1 H). Anal. (C₃₀H₂₉N₅O₄·0.3H₂O) C, H, N.

Compound 3. ¹H NMR (300 MHz, 10:1 CD₂Cl₂/CD₃OD): δ 1.88 (m, 4 H), 3.43 (t, *J* = 6.4 Hz, 2 H), 3.54 (t, *J* = 6.3 Hz, 2 H), 3.83 (s, 3 H), 4.44 (d, *J* = 5.9 Hz, 2 H), 6.94 (dt, *J* = 9.1, 2.2 Hz, 2 H), 7.22–7.34 (m, 6 H), 7.36 (dt, *J* = 9.2, 2.2 Hz, 2 H), 7.48 (dt, *J* = 8.8, 2.0 Hz, 2 H), 7.71 (dt, *J* = 8.8, 1.9 Hz, 2

H), 8.02 (bt, 1 H), 9.16 (s, 1 H). Anal. (C₃₀H₂₉N₅O₄·0.6H₂O) C, H, N.

Compound 4. ¹H NMR (300 MHz, CDCl₃): δ 3.84 (s, 3 H), 4.47 (d, *J* = 5.9 Hz, 2 H), 6.38 (d, *J* = 8.4 Hz, 1 H), 6.58 (bt, *J* = 5.7 Hz, 1 H), 6.94 (d, *J* = 9.1 Hz, 2 H), 7.20–7.40 (m, 18 H), 7.53 (d, *J* = 8.4 Hz, 1 H). Anal. (C₃₂H₂₈N₄O₃·0.2H₂O) C, H, N.

Compound 5. ¹H NMR (300 MHz, acetone-*d*₆): δ 0.90 (d, *J* = 6.6 Hz, 6 H), 1.82–2.00 (m, 5 H), 2.86 (bd, 2 H), 3.47 (bq, 4 H), 3.83 (s, 3 H), 7.00 (d, *J* = 8.8 Hz, 2 H), 7.38 (s, 1 H), 7.42 (d, *J* = 8.8 Hz, 2 H), 7.51 (d, *J* = 8.8 Hz, 2 H), 7.75 (bt, 1 H), 7.77 (d, *J* = 8.4 Hz, 2 H), 9.95 (s, 1 H). Anal. (C₂₇H₃₁N₅O₄·0.4H₂O) C, H, N.

Compound 6. ¹H NMR (300 MHz, CD₂Cl₂): δ 1.46 (m, 1 H), 1.78–1.95 (m, 8 H), 3.28 (m, 1 H), 3.37–3.61 (bm, 5 H), 3.70 (dd, *J* = 6.6, 7.0 Hz, 1 H), 3.79 (m, 1 H), 3.82 (s, 3 H), 3.96 (m, 1 H), 6.93 (d, *J* = 9.2 Hz, 2 H), 7.31 (bt, *J* = 5.7 Hz, 1 H), 7.35 (d, *J* = 9.2 Hz, 2 H), 7.42 (d, *J* = 8.8 Hz, 2 H), 7.48 (s, 1 H), 7.65 (d, *J* = 8.4 Hz, 2 H), 9.59 (s, 1 H). Anal. (C₂₈H₃₁N₅O₅·0.6H₂O) C, H, N.

Compound 7. ¹H NMR (300 MHz, DMSO-*d*₆): δ 4.40 (d, *J* = 6.3 Hz, 2 H), 7.17–7.27 (m, 6 H), 7.53 (s, 4 H), 7.55 (s, 1 H), 7.67 (d, *J* = 8.8 Hz, 2 H), 7.79 (d, *J* = 8.8 Hz, 2 H), 7.83 (bs, 1 H), 9.01 (bt, *J* = 5.0 Hz, 1 H), 10.70 (s, 1 H). Anal. (C₂₅H₂₀N₅O₃Cl·0.2H₂O) C, H, N.

Compound 8. ¹H NMR (300 MHz, acetone-*d*₆): δ 4.59 (d, *J* = 6.2 Hz, 2 H), 7.11 (tt, *J* = 1.7, 7.3 Hz, 1 H), 7.19–7.38 (m, 7 H), 7.45 (s, 1 H), 7.48–7.59 (m, 4 H), 7.72 (d, *J* = 8.1 Hz, 2 H), 8.32 (bt, 1 H), 9.78 (s, 1 H). Anal. (C₂₉H₁₉N₄O₂Cl·0.6H₂O) C, H, N.

Compound 9. ¹H NMR (300 MHz, CD₂Cl₂): δ 1.55 (m, 2 H), 1.68 (m, 3 H), 2.35 (s, 2 H), 3.09 (m, 3 H), 4.59 (d, *J* = 6.3 Hz, 2 H), 6.89 (d, *J* = 8.8 Hz, 2 H), 7.29 (dd, *J* = 4.7, 7.7 Hz, 1 H), 7.35 (s, 1 H), 7.42–7.47 (m, 6 H), 7.71 (dt, *J* = 8.1, 1.8 Hz, 1 H), 7.76 (t, *J* = 6.2 Hz, 1 H), 8.45 (dd, *J* = 1.5, 4.7 Hz, 1 H), 8.53 (s, 1 H), 9.45 (s, 1 H). Anal. (C₂₈H₂₇N₆O₂Cl) C, H, N.

Compound 10. ¹H NMR (300 MHz, CDCl₃): δ 0.89 (d, *J* = 6.6 Hz, 6 H), 1.84 (m, 1 H), 3.15 (t, *J* = 6.6 Hz, 2 H), 4.61 (d, *J* = 6.2 Hz, 2 H), 6.65 (bt, 1 H), 7.24–7.41 (m, 11 H). Anal. (C₂₂H₂₃N₄O₂Cl·0.3H₂O) C, H, N.

Compound 11. ¹H NMR (300 MHz, 10:1 CDCl₃/CD₃OD): δ 4.55 (d, *J* = 6.2 Hz, 2 H), 7.12 (t, *J* = 7.3 Hz, 1 H), 7.20–7.30 (m, 3 H), 7.41 (s, 4 H), 7.51 (t, *J* = 5.2 Hz, 1 H), 7.58 (m, 3 H), 7.65 (s, 1 H), 8.49 (bs, 2 H), 9.16 (s, 1 H). Anal. (C₂₃H₁₈N₅O₂Cl·1.0H₂O) C, H, N.

Compound 12. ¹H NMR (300 MHz, acetone-*d*₆): δ 2.26 (s, 3 H), 4.54 (d, *J* = 4.0 Hz, 2 H), 7.08–7.13 (m, 3 H), 7.24 (d, *J* = 8.1 Hz, 2 H), 7.32 (m, 2 H), 7.45 (s, 1 H), 7.46–7.59 (m, 4 H), 7.72 (d, *J* = 8.4 Hz, 2 H), 8.20 (bt, 1 H), 9.78 (s, 1 H). Anal. (C₂₅H₂₁N₄O₂Cl) C, H, N.

Compound 13. ¹H NMR (300 MHz, acetone-*d*₆): δ 3.81 (s, 3 H), 4.59 (d, *J* = 6.6 Hz, 2 H), 6.98 (d, *J* = 9.2 Hz, 2 H), 7.07 (t, *J* = 7.3 Hz, 1 H), 7.24–7.31 (m, 3 H), 7.35 (s, 1 H), 7.41 (d,

$J = 9.1$ Hz, 2 H), 7.68 (d, $J = 8.4$ Hz, 2 H), 7.75 (d, $J = 8.4$ Hz, 1 H), 8.35 (bt, 1 H), 8.41 (dd, $J = 1.8, 4.7$ Hz, 1 H), 8.58 (s, 1 H), 9.64 (bs, 1 H). Anal. ($C_{24}H_{21}N_5O_3 \cdot 0.4H_2O$) C, H, N.

Acknowledgment. We thank the Wilmington analytical chemistry group for their invaluable support in both the purification and the analysis of the libraries discussed above.

Supporting Information Available: Charts containing graphs of percent inhibition (at 10 μ M compound concentration) vs R^AR^B side chains for libraries 2 and 3, Scheme 4 showing the solution phase synthesis of compound 7, and a detailed description of methods used for protein expression and purification. This material is available free of charge via the Internet at <http://pubs.acs.org>.

References

- Covacci, A.; Telford, J. L.; Giudice, G. D.; Parsonnet, J.; Rappuoli, R. *Helicobacter pylori* Virulence and Genetic Geography. *Science* **1999**, *284*, 1328–1333.
- McGowan, C. C.; Cover, T. L.; Blaser, M. J. *Helicobacter pylori* and Gastric Acid: Biological and Therapeutic Implications. *Gastroenterology* **1996**, *110*, 426–438.
- Copeland, R. A.; Davis, J. P.; Dowling, R. L.; Lombardo, D.; Murphy, K. B.; Patterson, T. A. Recombinant Human Dihydroorotate Dehydrogenase: Expression, Purification, and Characterization of a Catalytically Functional Truncated Enzyme. *Arch. Biochem. Biophys.* **1995**, *323*, 79–86.
- Björnberg, O.; Rowland, P.; Larsen, S.; Jensen, K. F. Active Site of Dihydroorotate Dehydrogenase A from *Lactococcus lactis* Investigated by Chemical Modification and Mutagenesis. *Biochemistry* **1997**, *36*, 16197–16205.
- Rowland, P.; Nielsen, F. S.; Jensen, K. F.; Larsen, S. The Crystal Structure of the Flavin Containing Enzyme Dihydroorotate Dehydrogenase A from *Lactococcus lactis*. *Structure* **1997**, *5*, 239–252.
- Copeland, R. A.; Marcinkeviciene, J.; Haque, T. S.; Kopcho, L. M.; Jiang, W.; Wang, K.; Ecret, L. D.; Sizemore, C.; Amsler, K. A.; Foster, L.; Tadesse, S.; Combs, A. P.; Stern, A. M.; Trainor, G. L.; Slee, A.; Rogers, M. J.; Hobbs, F. *Helicobacter pylori*-selective Antibacterials Based on Inhibition of Pyrimidine Biosynthesis. *J. Biol. Chem.* **2000**, *275*, 33373–33378.
- Tomb, J.-F.; White, O.; Kerlavage, A. R.; Clayton, R. A.; Sutton, G. G.; Fleischmann, R. D.; Ketchum, K. A.; Klenk, H. P.; Gill, S.; Dougherty, B. A.; Nelson, K.; Quackenbush, J.; Zhou, L.; Kirkness, E. F.; Peterson, S.; Loftus, B.; Richardson, D.; Dodson, R.; Khalak, H. G.; Glodek, A.; McKenney, K.; Fitzgerald, L. M.; Lee, N.; Adams, M. D.; Hickey, E. K.; Berg, D. E.; Cocayne, J. D.; Utterback, T. R.; Peterson, J. D.; Kelley, J. M.; Cotton, M. D.; Weidman, J. M.; Fujii, C.; Bowman, C.; Watthey, L.; Wallin, E.; Hayes, W. S.; Borodovsky, M.; Karp, P. D.; Smith, H. O.; Fraser, C. M.; et al. The complete genome sequence of the gastric pathogen *Helicobacter pylori*. *Nature (London)* **1997**, *388*, 539–547.
- Alm, R. A.; Ling, L.-S. L.; Moir, D. T.; King, B. L.; Brown, E. D.; Doig, P. C.; Smith, D. R.; Noonan, B.; Guild, B. C.; DeJonge, B. L.; Carmel, G.; Tummino, P. J.; Caruso, A.; Uria-Nickelsen, M.; Mills, D. M.; Ives, C.; Gibson, R.; Merberg, D.; Mills, S. D.; Jiang, Q.; Taylor, D. E.; Vovis, G. F.; Trust, T. J. Genomic-sequence comparison of two unrelated isolates of the human gastric pathogen *Helicobacter pylori*. *Nature (London)* **1999**, *397*, 176–180.
- Chen, S. F.; Perrella, F. W.; Behrens, D. L.; Papp, L. M. Inhibition of Dihydroorotate Dehydrogenase Activity by Brequinar Sodium. *Cancer Res.* **1992**, *52*, 3521–3527.
- Marcinkeviciene, J.; Rogers, M. J.; Kopcho, L.; Jiang, W.; Wang, K.; Murphy, D. J.; Lippy, J.; Link, S.; Chung, T. D. Y.; Hobbs, F.; Haque, T.; Trainor, G. L.; Slee, A.; Stern, A. M.; Copeland, R. A. Selective Inhibition of Bacterial Dihydroorotate Dehydrogenases by Thiadiazolidinediones. *Biochem. Pharmacol.* **2000**, *60*, 339–342.
- Cherwinski, H. M.; Cohn, R. G.; Cheung, P.; Webster, D. J.; Xu, Y.-Z.; Caulfield, J. P.; Young, J. M.; Nakano, G.; Ransom, J. T. The immunosuppressant leflunomide inhibits lymphocyte proliferation by inhibiting pyrimidine biosynthesis. *J. Pharmacol. Exp. Ther.* **1995**, *275*, 1043–1049.
- Davis, J. P.; Cain, G. A.; Pitts, W. J.; Magolda, R. L.; Copeland, R. A. The Immunosuppressive Metabolite of Leflunomide Is a Potent Inhibitor of Human Dihydroorotate Dehydrogenase. *Biochemistry* **1996**, *35*, 1270–1273.
- Lee, A.; O, R. J.; De, U. M.; Robertson, B.; Daskalopoulos, G.; Dixon, M. A Standardized Mouse Model of *Helicobacter pylori* Infection: Introducing the Sydney Strain [published erratum appears in *Gastroenterology* **1997**, *113*(2), 732]. *Gastroenterology* **1997**, *112*, 1386–1397.
- Wehrli, W. Rifampin: Mechanisms of Action and Resistance. *Rev. Infect. Dis.* **1983**, *5* (Suppl. 3), S407–S411.
- Davis, J. P.; Copeland, R. A. Histidine to Alanine Mutants of Human Dihydroorotate Dehydrogenase. *Biochem. Pharmacol.* **1997**, *54*, 459–465.
- Turnbough, C. J.; Bochner, B. Toxicity of the Pyrimidine Biosynthetic Pathway Intermediate Carbamyl Aspartate in *Salmonella typhimurium*. *J. Bacteriol.* **1985**, *163*, 500–505.
- Gustafson, G.; Davis, G.; Waldron, C.; Smith, A.; Henry, M. Identification of a New Antifungal Target Site Through a Dual Biochemical and Molecular-Genetics Approach. *Curr. Genet.* **1996**, *30*, 159–165.
- Liu, S.; Neidhardt, E.; Grossman, T.; Ocain, T.; Clardy, J. Structures of Human Dihydroorotate Dehydrogenase in Complex with Antiproliferative Agents. *Struct. Fold Des.* **2000**, *8*, 25–33.
- Lam, P. Y.; Clark, C. G.; Dominguez, C.; Fevig, J. M.; Han, Q.; Li, R.; Pinto, D. J.-P.; Pruitt, J. R.; Quan, M. L. Preparation of novel guanidine mimics as factor Xa inhibitors. In *PCT Int. Appl.* (The Du Pont Merck Pharmaceutical Company, U.S.A.), WO 1998; pp 268.
- Ashton, W. T.; Doss, G. A. A Regioselective Route to 3-Alkyl-1-aryl-1H-pyrazole-5-carboxylates: Synthetic Studies and Structural Assignments. *J. Heterocycl. Chem.* **1993**, *30*, 307–311.
- Danishefsky, S. J.; Pearson, W. H.; Segmuller, B. E. Total Synthesis of (±)-3-Deoxy-D-manno-2-octulopyranosate (KDO). *J. Am. Chem. Soc.* **1985**, *107*, 1280–1285.
- Robbins Scientific Corporation, Sunnyvale, CA.
- Rijkers, D. T. S.; Adams, H. P. H. M.; Hemker, H. C.; Tesser, G. I. A Convenient Synthesis of Amino Acid *p*-Nitroanilides; Synthons in the Synthesis of Protease Substrates. *Tetrahedron* **1995**, *51*, 11235–11250.
- Kabalka, G. W.; Deshpande, S. M.; Wadgaonkar, P. P.; Chatla, N. The Transformation of Nitriles into Amides using Sodium Percarbonate. *Synth. Commun.* **1990**, *20*, 1445–1451.

JM020112W